Iranica Journal of Energy & Environment 4 {(1) Special Issue on Nanotechnology}: 49-52, 2013
ISSN 2079-2115
IJEE an Official Peer Reviewed Journal of Babol Noshirvani University of Technology
DOI: 10.5829/idosi.ijee.2013.04.01.41138

BUT

# Ni-Doped $SnO_2$ Nanoparticles Synthesized by Chemical Co-Precipitation Method

*M. Aliahmad and M. Dehbashi*

[1]Department of Physics, Faculty of sciences, University of Sistan and Baluchestan, Zahedan, Iran
[2]Department of Physics, Faculty of sciences, University of Zabol, Zabol, Iran

(Received: August 15, 2012; Accepted in Revised Form: February 4, 2013)

**Abstract:** Ni-doped $SnO_2$ nanocrystalline powders have been synthesized by the co-precipitation method from $SnCl_2.2H_2O$ and $NiCl_2.6H_2O$. Nanoparticles crystallize in lower temperature (350°C) and shorter time (2hours) respect to other methods. The samples have been characterized by various advanced techniques such as, X-ray diffraction (XRD), Fourier transform infrared spectroscopy (FT-IR), Transmission electron microscopy (TEM) and Vibrating sample magnetometer (VSM). The X-ray diffraction reveals that all samples are pure rutile-type tetragonal phase and the average particles size was observed to vary from 32 nm to 24 nm as the nickel content was increased, The TEM images confirms the size of tin oxide particles in nanoscale and VSM measurements indicate that Ni-doped samples have superparamagnetic properties and they are single-domain nanoparticles.

**Key words:** Nanoparticles · Nickel · Tin oxide · Superparamagnetic

## INTRODUCTION

In recent years, the interest in the physical properties of semiconducting metal oxide, such as $SnO_2$, $TiO_2$ and ZnO, has significantly increased due to their potential applications, in special when they are intentionally doped with magnetic elements. Tin oxide ($SnO_2$) with a wide-band-gap n-type semiconductor (3.6eV at 300°K), known as one of the most widely used semiconducting oxides due to its chemical and mechanical stabilities. It has been widely studied over decades because of its most applications in various optoelectronic devices, transparent electrodes and sensors [1-3].The properties of $SnO_2$ nanostructures can be enhanced by several ways like impurity doping [4], coating with surfactants [5] and annealing [6]. The final properties of impurity doped $SnO_2$ nanoparticles are related to both composition and processing method. Nanoparticles of tin oxide have been synthesized through different chemical routes, such as co-precipitation[7], hydrothermal [8] and sol-gel [9] methods among others. In this work, we synthesized Ni-$SnO_2$ nanoparticles by chemical coprecipitation method because this method has some advantages such as precise control over the stoichiometry, low temperature synthesis, high purity and high chemical homogeneity.

## MATERIALS AND METHODS

Ni doped $SnO_2$ nanoparticles have been synthesized by chemical co-precipitation method, $SnCl_2.2H_2O$ (98% Merck, Germany) and $NiCl_2.6H_2O$ (98% Merck) have been used as starting materials for the synthesis of Ni doped $SnO_2$ nanoparticles. The required amounts of $SnCl_2.2H_2O$ and $NiCl_2.6H_2O$ were added to double-distilled water and dissolved. Then, an aqueous ammonia (1M) was dropped into the mixture solution with constant stirring at 30°C until a pH of 5 reached. The resulting precipitate were collected, washed with distilled water and then dried at 100°C for several hours. Heating treatments of the synthesized nano-powders were conducted at 350°C for 2 hours. The preparation process of Ni-doped $SnO_2$ nanocrystalline powders is shownin Figure 1. Crystallanity, structure and particle size of Ni-doped $SnO_2$ nanoparticles were determined by X-ray diffraction (XRD) using Rigaku-Miniflex X-ray diffractometer with CuK$\alpha$ radiations ($\lambda$ =0.15406 nm) in 2$\theta$ range from 10° to 70°.

**Corresponding Author:** M. Aliahmad, Department of Physics, Faculty of sciences, University of Sistan and Baluchestan, Zahedan, Iran. Tel/Fax: +985412446565, E-mails: aliahmad@phys.usb.ac.ir.

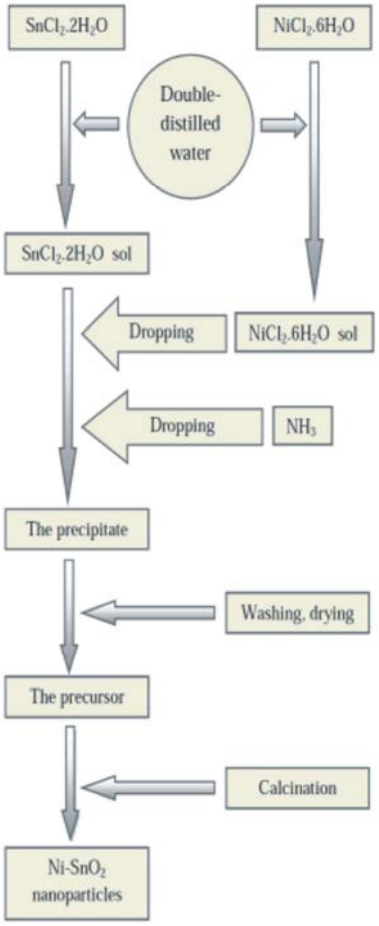


Fig. 1: The preparation process schema of Ni-$SnO_2$ nanoparticles

Morphologies and particle sizes of the samples were observed with a Hitachi H-800 transmission electron microscope (TEM), FTIR spectrum was recorded in the range 400-4000 $cm^{-1}$ on a FTIR 460-plus spectrophotometer using KBr pellets. The magnetic measurements were obtained using a Vibrating Sample Magnetometer (VSM) in the room temperature.

## RESULTS AND DISCUSION

XRD patterns of $Sn_{1-x}Ni_xO_2$ (with x = 0, 0.01 and 0.02) annealed at 350°C for 2 h are shown in Figure 2, in which $S_1$, $S_2$ and $S_3$ correspond to x = 0, 0.01 and 0.02, respectively. All diffraction peaks are well assigned to tetragonal crystalline phase of tin oxide (with the reference pattern JCPDS 880287) and the Ni doping does not change the tetragonal structure of $SnO_2$. From Figure 2, it is noted that the intensity of the $Sn_{1-x}Ni_xO_2$

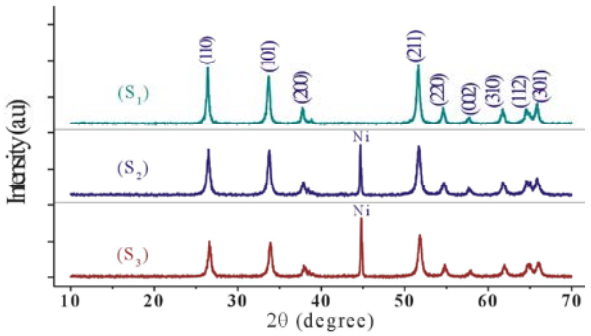


Fig. 2: XRD patterns of ($S_1$) $SnO_2$, ($S_2$) $Sn_{0.99}Ni_{0.01}O_2$ and ($S_3$) $Sn_{0.98}Ni_{0.02}O_2$ nanoparticles

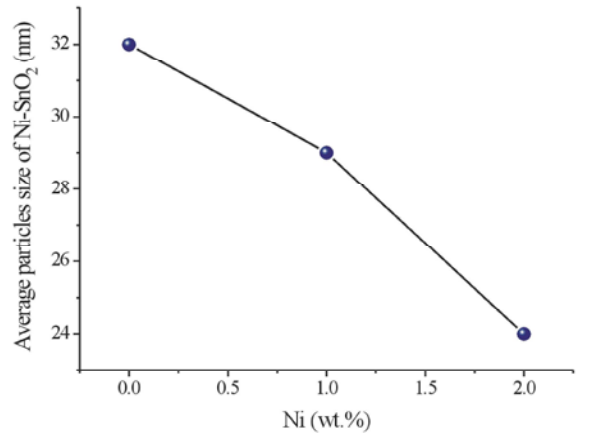


Fig. 3: The effect of the Ni-doping quantities on the average particle size of Ni-$SnO_2$ nanocrystalline powders

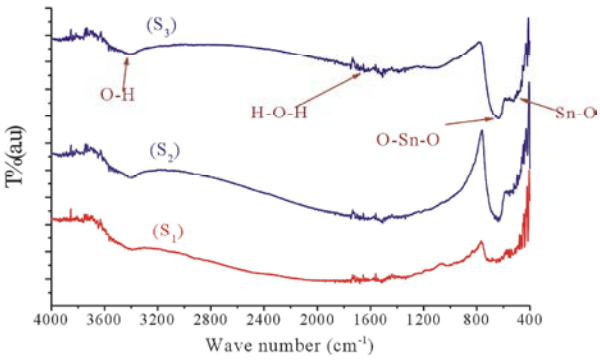


Fig. 4: FT-IR spectra of ($S_1$) $SnO_2$, ($S_2$) $Sn_{0.99}Ni_{0.01}O_2$ and ($S_3$) $Sn_{0.98}Ni_{0.02}O_2$ nanoparticles

peaks decreases with increasing Ni content and the full-width at half-maximum (FWHM)of the peaks increases with increasing Ni content, as well indicates that average particle size of samples decreases gradually as the Ni content increases (Figure 3). The average particle size of samples are calculated using Scherrer's formula,

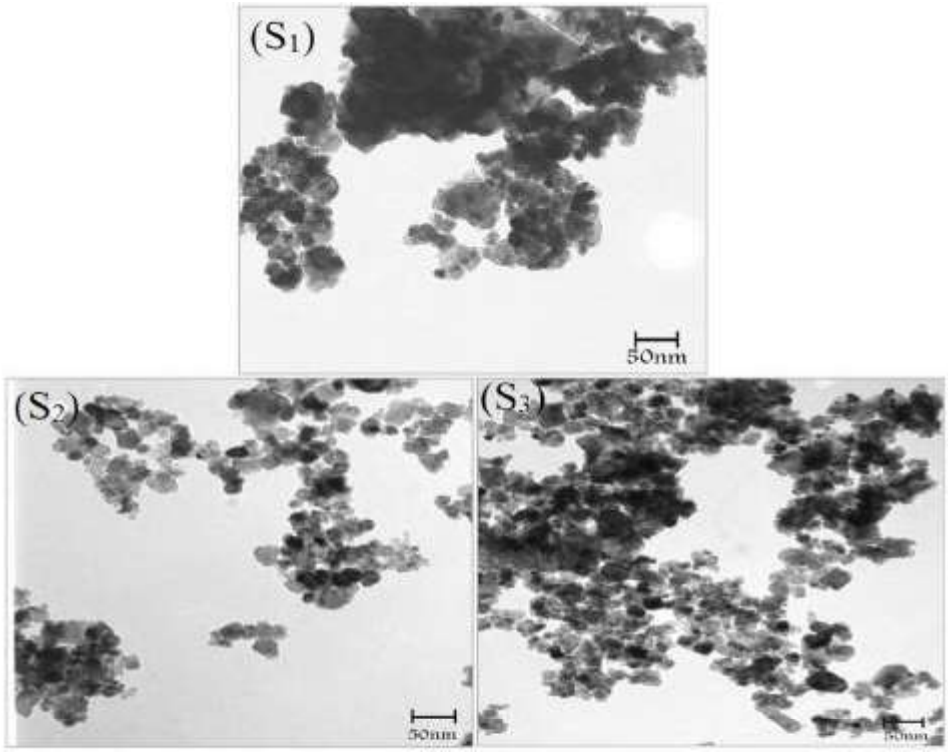


Fig. 5: TEM images of ($S_1$) $SnO_2$, ($S_2$) $Sn_{0.99}Ni_{0.01}O_2$ and ($S_3$) $Sn_{0.98}Ni_{0.02}O_2$ nanoparticles

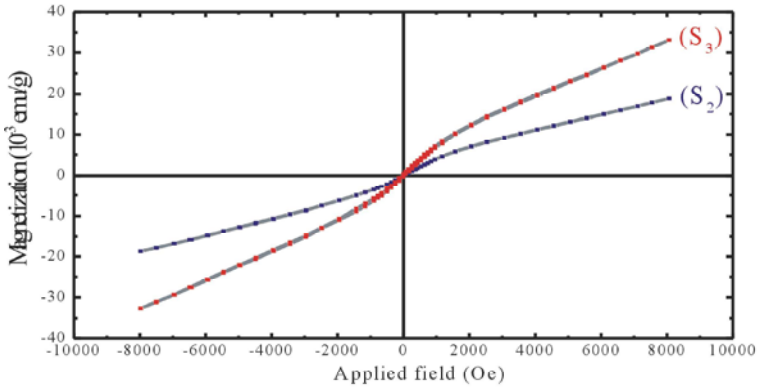


Fig. 6: Room temperature hysteresis curves of ($S_2$) $Sn_{0.99}Ni_{0.01}O_2$ and ($S_3$) $Sn_{0.98}Ni_{0.02}O_2$ nanoparticles

$$D = \frac{0.9\lambda}{\beta\cos(\theta)}$$

where $\lambda$ is the wavelength of CuK$\alpha$ radiation (= 0.154056 nm), $\beta$ is the full width at half maximum (FWHM) of the (*hkl*) peak at the diffracting angle $2\theta$ [10], all the peaks are used to calculate the average particle size of samples.

The average particles size of samples are found to be 32nm for sample $S_1$, 29 nm for sample $S_2$ and 24nm for sample $S_3$ by using scherrer's formula.

The FT-IR transmittance spectra of different samples are given in Figure 4, in which the band located at 3398 $cm^{-1}$ is owing to the vibration of O-H and the band located at 1636 $cm^{-1}$ is due to the H-O-H vibrating mode of the absorbed water, while the bands at around 528 and 643 $cm^{-1}$ can be attributed to the Sn-O stretching vibration and the O-Sn-O blending vibration in $SnO_2$.

TEM images of ($S_1$) $SnO_2$, ($S_2$) $Sn_{0.99}Ni_{0.01}O_2$ and ($S_3$) $Sn_{0.98}Ni_{0.02}O_2$ nanoparticles calcined at 350°C for 2 hours are shown in Figure 5. It is shown that the powders are uniform in size and the particle size of samples decreases with increasing doping quantities of Ni. The particle shape of the samples is spherical with an average diameter

of 28 nm for pure $SnO_2$, 25 nm for 1% Ni-doped $SnO_2$ and 21 nm for 2% Ni-doped $SnO_2$. The results of average particle size measurement from TEM observations are having good agreement with the XRD line broadening method.

To probe the magnetic properties of $Sn_{0.99}Ni_{0.01}O_2$ and $Sn_{0.98}Ni_{0.02}O_2$ nanoparticles, room temperature magnetization is performed on the samples and is shown in Figure 6. It shows no hysteresis loops and the magnetization curve exhibits zero remanence and coercivity (the coercive field is the applied magnetic field that needs to be applied in the direction opposite the initial magnetic field, to bring the magnetization back to zero), which proves that nanoparticles have superparamagnetic properties and they are single-domain nanoparticles [11, 12]. The superparamagnetism enables the nanoparticles to respond to an applied magnetic field without any permanent magnetization and redisperse rapidly when the magnetic field is removed. In the Figure 6, it can be also observed that magnetization of samples increases with increasing doping quantities of Ni.

## CONCLUSIONS

Ni-doped $SnO_2$ nanocrystalline powders were synthesized by the co-precipitation method from $SnCl_2.2H_2O$ and $NiCl_2.6H_2O$. XRD results show that the average particles size is in the range from 24 to 32 nm, it is shown that the average particles size of the nanoparticles decreases with increasing amounts of doping Ni and nanoparticles have pure rutile structure, TEM images of $SnO_2$ and Ni-$SnO_2$ powders shows that the particle shape of the samples is spherical with an average diameter of 28 nm for pure $SnO_2$, 25 nm for 1% Ni-doped $SnO_2$ and 21 nm for 2% Ni-doped $SnO_2$, confirming the reduction in particles size as a result of Ni doping in $SnO_2$. Particles size obtained from TEM analysis is comparable with average particles size calculated from XRD spectra and VSM measurements of nickel doped $SnO_2$ nanoparticles indicates that both samples $Sn_{0.99}Ni_{0.01}O_2$ and $Sn_{0.98}Ni_{0.02}O_2$ have superparamagnetic properties and they are single-domain nanoparticles.

## REFERENCES


1. Vishwakarma, S.R., Rahmatullah and H.C. Prasad, 1993. Low Cost $SnO_2$:P/$SiO_2$/n-Si (Textured) Heterojunction Solar Cells. Journal of Physics D., 26: 959-962.
2. Lalauze, R., J.C. Le Thiesse, C. Pijolat and M. Soustelle, 1987. $SnO_2$Gas Sensor. Effect of $SO_2$Treatment on TheElectrical Properties of $SnO_2$. Solid State Ionics, 12: 453-457.
3. Hidalgo, P., R.H.R. Castro, A.C.V. Coelho and D. Gouvêa, 2005. Surface Segregation and Consequent $SO_2$ Sensor Response in $SnO_2$ - NiO. Chemistry of Materials Journal, 17: 4149-4153.
4. Cabrera, A.F., A.M. Mudarra Navarro, C.E. Rodríguez Torres and F.H. Sánchez, 2007. Mechanosynthesis of Fe-doped $SnO_2$ Nanoparticles. Physica B., 398: 215-218.
5. Khun Kamalpreet, K., A. Mahajan and R.K. Bedi, 2011. Effect of Cationic/Anionic Organic Surfactants on Evaporation Induced Self-Assembled Tin Oxide Nanostructured Films. Applied Surface Science, 257: 2929-2934.
6. Cukrov, M.L., T. Tsuzuki and P.G. McCormick, 2000. $SnO_2$ Nanoparticles Prepared by Mechanochemical Processing. Scripta Materialia, 44: 1787-1790.
7. Ricardo, H.R. Castro, P. Hidalgo, R. Muccillo and D. Gouvea, 2003. Microstructure and Structure of NiO-$SnO_2$and $Fe_2O_3$-$SnO_2$systems.Applied Surface Science, 214: 172-177.
8. Baik, N.S., G. Sakai, N. Miura and N. Jamazoe, 2000. Preparation of Stabilized NanosizedTin Oxide Particles by Hydrothermal Treatment.Journal of the American Ceramic Society, 83: 2983-2987.
9. Siciliano, P., 2000. Preparation, Characterization andApplication of Thin Films for Gas Sensors Prepared by Cheap Chemical Method. Sensors and Actuators B., 70: 153-164.
10. Patterson, A.L., 1939. The Scherrer Formula for X-ray Particle Size Determination. Physical Review Online Archives (PROLA), 56: 978-982.
11. Zhiya, M.A., G. Yueping and H. Liu, 2005. Synthesis and Characterization of Micron-Sized Monodisperse Superparamagnetic Polymer Particles with Amino Groups. Journal of Polymer Science Part A: Polymer Chemistry, 43: 3433-3439.
12. Ashby, M.F., P.J. Ferreira and D. L.Schodek, 2009. Nanomaterials, Nanotechnologies and Design an Introduction for Engineers and Architects. Butterworth-Heinemann Publication.